frontiers | Frontiers in Energy Research

TYPE Original Research
PUBLISHED 07 February 2023
DOI 10.3389/fenrg.2023.1114512

Check for updates

OPEN ACCESS

EDITED BY
Chuanchang Li,
Changsha University of Science and Technology, China

REVIEWED BY
Solomon Giwa,
Olabisi Onabanjo University, Nigeria
Collins Nwaokocha,
Olabisi Onabanjo University, Nigeria

*CORRESPONDENCE
U. O. Uyor,
UyorUO@tut.ac.za

SPECIALTY SECTION
This article was submitted to Process and Energy Systems Engineering, a section of the journal Frontiers in Energy Research

RECEIVED 02 December 2022
ACCEPTED 27 January 2023
PUBLISHED 07 February 2023

CITATION
Uyor UO, Popoola API and Popoola OM (2023), Flexible dielectric polymer nanocomposites with improved thermal energy management for energy-power applications.
Front. Energy Res. 11:1114512.
doi: 10.3389/fenrg.2023.1114512

COPYRIGHT
© 2023 Uyor, Popoola and Popoola. This is an open-access article distributed under the terms of the Creative Commons Attribution License (CC BY). The use, distribution or reproduction in other forums is permitted, provided the original author(s) and the copyright owner(s) are credited and that the original publication in this journal is cited, in accordance with accepted academic practice. No use, distribution or reproduction is permitted which does not comply with these terms.

Flexible dielectric polymer nanocomposites with improved thermal energy management for energy-power applications

U. O. Uyor[1,2]*, A. P. I. Popoola[1] and O. M. Popoola[2,3]

[1]Department of Chemical, Metallurgical and Materials Engineering, Tshwane University of Technology, Pretoria, South Africa, [2]Center for Energy and Electric Power, Tshwane University of Technology, Pretoria, South Africa, [3]Department of Electrical Engineering, Tshwane University of Technology, Pretoria, South Africa

Most polymer materials are thermal and electrical insulators, which have wide potential in advanced energy-power applications including energy conversion. However, polymers get softened when in contact with heat, which causes their molecular chains to flow as the temperature increases. Although polymer dielectrics exhibit high power density, they face challenges of low energy density which is due to the low dielectric permittivity associated with them. Therefore, this study tried to address the poor thermal energy management and low energy density of poly (vinylidene fluoride) (PVDF) while maintaining its flexible property using low content of hybrid carbon nanotubes (CNTs–0.05wt%, 0.1wt%) and boron nitride (BN–5wt%, 10wt%) nano-reinforcements. The nanocomposites were developed through solvent mixing and hot compression processes. The dielectric constant increased from 9.1 for the pure PVDF to 42.8 with a low loss of about 0.1 at 100 Hz for PVDF-0.1wt%CNTs-10wt%BN. The thermal stability of the nanocomposites was enhanced by 55°C compared to the pure PVDF. The nanocomposites also showed improved melting and crystallization temperatures. The developed PVDF-CNTs-BN nanocomposites showed significant enhancements in thermal energy management, stability, and dielectric properties. The significantly improved properties are credited to the synergetic effects between CNTs and BN in the PVDF matrix in promoting homogeneous dispersion, thermal barrier, interfacial polarization/bonding, insulative and conductive properties. Therefore, the developed nanomaterials in this study can find advanced applications in the energy-power sector owing to their enhanced performances.

KEYWORDS

boron nitride, dielectric properties, thermal stability, PVDF (polyvinyliden fluoride), CNTS (carbon nanotube)

1 Introduction

Polymer materials are constantly developing and appealing issue in a variety of scientific fields, including material engineering, electro-technology, and even biomedical applications. Polymer-based nanocomposites have gained increasing attention due to their improved thermal properties, mechanical flexibility, fatigue reliability, and ease of production. Fluoropolymers such as poly (vinylidene fluoride) (PVDF) has gained attention as dielectric energy storage material in recent years (Wang et al., 2018a; Karaphun et al., 2021; Adaval et al., 2022a; Adaval et al., 2022b). PVDF is widely used as dielectric energy storage because of its good mechanical strength, thermal stability, strong dielectric strength, higher dielectric constant compared to other polymers. Polymer dielectrics possess the advantages of excellent flexibility, high dielectric

breakdown strength and good processability. Due to the desired power density and charging-discharging rate capabilities of dielectric materials (Xihong, 2013), they are commonly used in design of capacitors which convert electrostatic charges and store as electrical energy. They have found wide application in electronics and electric power systems. In comparison to other types of energy storage devices such as batteries, the dielectric capacitor is currently one of the most promising options due to its fast charge/discharge speed and high power density. The dielectric constant, loss and breakdown strength are intrinsic material parameters that describe the dielectric properties of a dielectric substance (Ye et al., 2018).

In addition, thermal conversation/dissipation and thermal stability are also required features of dielectric materials for advanced electric power application. However, polymer dielectric materials get softened when in contact with heat, which causes their molecular chains to flow as the temperature increases due to their poor thermal management (Uyor et al., 2019a). Although polymer dielectrics exhibit high power density, they face challenges of low energy density which is due to the low dielectric permittivity associated with them. However, there have been various efforts by different studies to address these challenges by incorporating large dielectric constant and high thermal property materials into the matrix of various polymer (Wang et al., 2018b; Jiang et al., 2018; Jin et al., 2019). For instance, Zhang et al. (2015) significantly enhanced thermal properties of a PVDF/CNTs by the addition of graphene oxide. Also, Maity et al. (2016) developed percolative polymer-graphene nanocomposites with improved dielectric properties.

Percolative polymer-based nanocomposites through experimental studies have shown characteristic of high dielectric constant materials up to 1×10^6 (Weng et al., 2017). This range of dielectric constant can be used to achieve significantly large energy density that can compete with electrochemical capacitors (Cortes and Phillips, 2015). High dielectric loss, energy dissipation, and poor breakdown strength, however, are the main obstacles preventing this class of polymer nanocomposites from being used in practical applications (Han et al., 2013). This is explained by significant current leakage, free electron mobility, and -orbital electrons. Additionally, pure polymers often have a poor thermal management (Jang et al., 2021), low dielectric constant and energy storage density (Uyor et al., 2019b). It is well known that a polymer film with a low dielectric constant restricts high energy storage capacity (Ye et al., 2019). However, various studies have tried to address these challenges using percolative conductive (such as graphene and carbon nanotubes) and insulative ceramic nanoparticles (Li et al., 2015; Du et al., 2016; Lakshmi et al., 2018). This high volume of ceramic nanoparticles often leads to deterioration of the flexibility and other mechanical properties of such polymer composites with difficulty in processing.

Therefore, utilizing modest concentrations of hybrid carbon nanotubes (CNTs) and boron nitride (BN), this study enhanced the thermal energy management, stability, and dielectric permittivity of PVDF while keeping its flexibility. PVDF is a semi crystalline material with good mechanical property, chemical resistance and ferroelectric properties (Wang et al., 2012). The CNTs is a 1D carbon-based nanomaterials with excellent mechanical, electrical and thermal properties. On the other hand, BN has a good thermal conductivity, insulative property, and breakdown strength. Although it has a low dielectric permittivity, it is preferred for this study due to its proximity in dielectric properties with the polymer to reduce localized electric field accumulation and sudden breakdown on the application of electric field. The generation of micro-capacitors by CNTs and BN in the PVDF matrix was the cause of the increased dielectric permittivity attained in this work. The increased thermal stability was a result of the uniform dispersion and good thermal properties of CNTs and BN, which were aided by the nanoparticles' various dimensional configurations. The fabricated nanocomposites provide the necessary characteristics for advanced dielectric energy-power applications and superior thermal management.

TABLE 1 Nanocomposites preparation concentrations.

S/N	CNTs (wt%)	BN (wt%)	Nanocomposites Denotation
1	0.00	0.00	Pure PVDF
2	0.05	5.00	PVDF-0.05wt%CNTs-5wt%BN
3	0.05	10.00	PVDF-0.05wt%CNTs-10wt%BN
4	0.10	5.00	PVDF-0.1wt%CNTs-5wt%BN
5	0.10	10.00	PVDF-0.1wt%CNTs-10wt%BN

2 Experimental section

2.1 Materials

Poly (vinylidene fluoride) (PVDF) (average molecular weight 534,000, density 1.74 g/mL at 25 C) and N, N-dimethyl formamide (DMF) (assay ≥99%) were purchased from Sigma-Aldrich, South Africa. Hexagonal boron nitride (BN) (assay >99.5%, particles size 100 nm, and density 2.2 g/mL at 25°C) and multi-walled carbon nanotubes (MWCNTs) (purity - >98%, diameter - 10–30 nm, length - 5–20 μm) were sourced from Hongwu International Group, China. All materials were used as received without any modification.

2.2 Nanocomposites fabrication

Solution mixing technique was used to produce the polymer nanocomposites. The various concentrations of CNTs and BN as shown in Table 1 were randomly mixed in beakers containing DMF to exfoliate the nanoparticles. The mixtures were ultrasonicated for 5 h (at high frequency, power of 300 W and temperature of 80°C). PVDF was mixed with DMF for 10 min while being magnetically stirred (at speed of 300 rpm and temperature of 80°C). The pre-dispersed PVDF was then added to the dispersed mixtures of CNTs and BN, which were then homogeneously mixed using stirrer for 3 h. Later, the nanocomposites were cast onto a clean glass plate and dried in an oven until the weights were constant. Using a carver press moulder, the nanocomposites were hot pressed to desired shape and size at temperature of 200°C and pressure of 10 MPa for 10 min. The nanocomposites developed in this study with different amounts of CNTs and BN are denoted as displaced in Table 1. Also, pure PVDF was also fabricated following similar steps as described above for comparison.

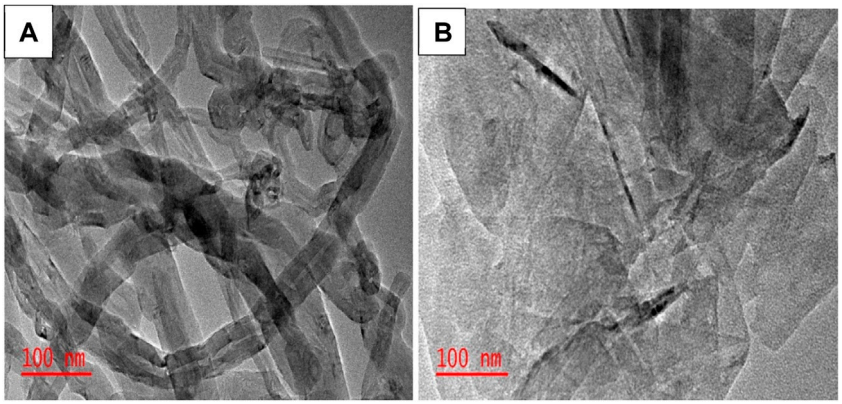

FIGURE 1
TEM micrographs of the **(A)** CNTs and **(B)** BN nanoparticles.

2.3 Nanocomposites characterization

A high-performance Scanning Electron Microscope (SEM) (VEGA 3 TESCAN) operating at accelerated voltage of 20 kV was used to evaluate the dispersion and morphology of the nanocomposites. The Transmission Electron Microscope (TEM) (JEM-2100) was used to examine the structures of the CNTs and BN at acceleration voltage 200 kV and beam current of 110 μA. X'pert PRO PANalytical diffractometer at 30 kV and 40 mA was used to study the diffraction patterns of the nanoparticles and nanocomposite materials. Utilizing a differential scanning calorimeter (DSC Q2000 with accuracy of ± 0.01°C), the melting and crystallization properties of the nanocomposites were studied in a nitrogen-filled atmosphere at a 10 C/min heating and cooling rate. The thermal stability of the nanocomposites was obtained using Thermogravimetry Analyzer (TGA) (TA instrument Q500 with accuracy of ± 1°C) at a heating rate of 10 C/min in a nitrogen environment. Capacitance and resistance of the nanocomposites were measured using an LCR meter (B&K 891 with accuracy of ± 0.05%) through a frequency range of 100 Hz to 10 kHz, from which the electrical conductivity, dielectric constant and loss of the nanocomposites were obtained. To prevent contact resistance, the nanocomposites films were coated with silver paste. By utilizing a high voltage transformer (Conelectric BS 3941 with accuracy of ± 1 V) at an applied rate of 50 V/min until failure, the dielectric breakdown strength of the nanocomposites was measured.

3 Results and discussion

3.1 Microstructural analysis

The microstructures of the CNTs and BN were examined using TEM as displayed in Figure 1. The CNTs has long in-plane dimension (Figure 1A), while the BN shows few stackings of nanoparticles' layers (Figure 1B). Interpenetration of CNTs and BN results in 3D dense network configurations in the polymer matrix since they are respectively 1D and 2D structural nanomaterials (Schmidt et al., 2002; Yu et al., 2016). Such 3D structures facilitate the enhancement of i) dielectric constant *via* micro-capacitors formation and ii) thermal properties *via* formation of conductive network structures. The presence of the plate-like structure of the insulative BN nanoparticles led to the reduction of the conductive network structures formation in the polymer matrix. The combination of different conductive and insulative nanoparticles enhances dielectric properties through formation of micro-capacitors in the polymer matrix. In addition, their different dimensional structures assisted each other in promoting dispersion in the polymer matrix. Both nanoparticles have good synergy and compatibility with each other since they are uniformly distributed in the polymer matrix as presented by the SEM micrographs in Figure 2.

Morphological structures of the developed PVDF-CNTs-BN nanocomposites are shown in Figure 2. Addition of foreign bodies in a polymer matrix often changes its microstructure and gives it new properties. This was noted in this study when CNTs and BN were incorporated into the PVDF matrix as compared to its pure state (Figure 2A). The morphologies of PVDF-CNTs-BN nanocomposites revealed good interaction and dispersion of the nanoparticles. All the nanocomposites showed dense microstructure due to the presence of the BN nanoparticles as displayed in Figures 2B–E. However, PVDF-0.1wt%CNTs-5wt%BN showed some visible CNTs due to the increase in content of CNTs from 0.05wt% to 0.1wt% with only 5wt% BN (Figure 2D). This can also be attributed to the high driving force in bringing the CNTs together at high content. In general, good dispersion of the CNTs and BN in the PVDF matrix was achieved. None of the nanocomposites generally displayed substantial microcracking or debonding of the nanoparticles from the matrix, indicating good compatibility with their constituents. The different dimensional structures of CNTs (1D) and BN (2D) assist each other in obtaining uniform dispersion in the PVDF matrix (Min et al., 2018). Where BN may have minimized the wall-to-wall interactions of CNTs and CNTs minimized the layers-layers interactions of BN nanoparticles. Although CNTs has high tendency of showing agglomeration in the polymer matrix due to its entanglement nature (see Figure 1A) and BN may show difficulty to intercalate with polymer molecular chain due to its layered structure, this was supressed by using them at relative low quantities as shown with SEM micrographs in Figure 2.

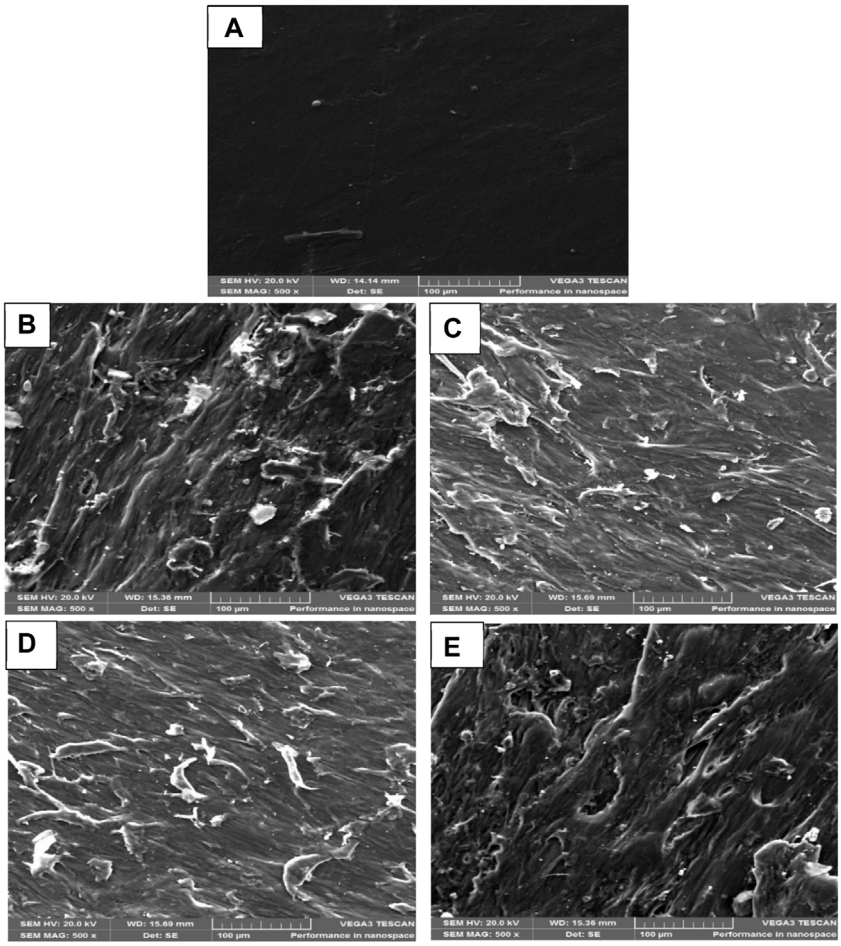

FIGURE 2
SEM Micrographs of the **(A)** pure PVDF **(B)** PVDF-0.05wt%CNTs-5wt%BN **(C)** PVDF-0.05wt%CNTs-10wt%BN **(D)** PVDF-0.1wt%CNTs-5wt%BN and **(E)** PVDF-0.1wt%CNTs-10wt%BN nanocomposites.

3.2 XRD analysis

This study further examined the crystal phases of the CNTs and BN using XRD after employing TEM analysis in determining their structural dimensions. The CNTs and BN have similar diffraction patterns as shown in Figure 3A, since they are both hexagonally organized nanoparticles. They typically have significant diffraction peaks at $2\theta = 26.4^{\circ}$ and 44.3°, which correspond to the crystal planes of (002) and (100), indicating graphitic crystal plane (Ouyang et al., 2014) and hexagonal BN (Ansaloni and de Sousa, 2013; Huang et al., 2013) respectively. While the diffraction peak at $2\theta = 54.5^{\circ}$ with crystal plane of (004) suggests a limited number of CNTs walls and BN stacking layers. The nanocomposites' XRD diffraction patterns were also examined as shown in Figure 3B. PVDF showed strong - phase intensity at $2\theta = 17.5^{\circ}$, 19.1°, 26.4° and a broad peak at $2\theta = 38^{\circ}$, corresponding to crystal plane of (100) (020) (021) and (040) respectively. The PVDF matrix showed predomination of α-phase. However, the broad peak significantly decreased upon inclusion of the CNTs and BN nanoparticles into the PVDF matrix. This can be attributed to the good interfacial bond and interaction between the PVDF and the nanoparticles. Comparing the diffraction patterns of the pure PVDF and the nanocomposites, no new diffraction peak was found. This indicates absence of new phase formation, but the phases predominated by the PVDF matrix. The reduction in the broad peak of the nanocomposites indicates increase in crystalline phase, which is caused by the addition of the nanoparticle. This indicates reduction in the amorphous phase of the PVDF with the addition of the CNTs and BN, which is vital for improvement of dielectric and piezoelectric properties (Fan et al., 2012).

3.3 DSC properties and thermal stability

The melting (T_m) and crystallization (T_c) Temperature of the nanocomposites from the DSC results are represented in Figure 4. The figure shows that all the nanocomposites required higher thermal energy to be melted compared to the pure PVDF. The larger T_m of the nanocomposites is an indicative of higher energy required in thermal breaking of the bonds between the PVDF matrix and the nanoparticles (He et al., 2014). This is due to the good interfacial interaction between the matrix and CNTs-BN, which gave the nanocomposites higher T_m. Therefore, T_m in the range of 160.73°C for the pure PVDF to optimal of about 169.6°C for PVDF-0.05wt%CNTs-10wt%BN were obtained

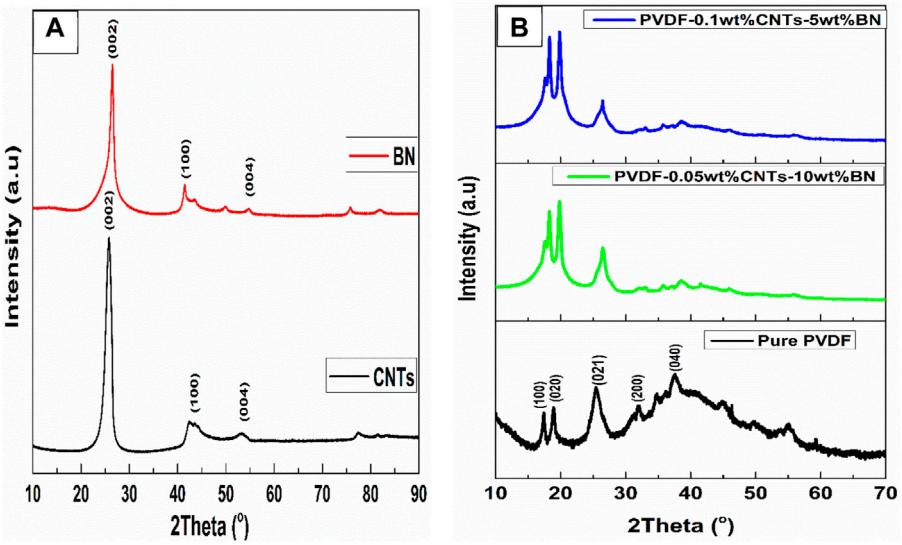

FIGURE 3
XRD diffraction patterns of the **(A)** nanoparticles and **(B)** nanocomposites.

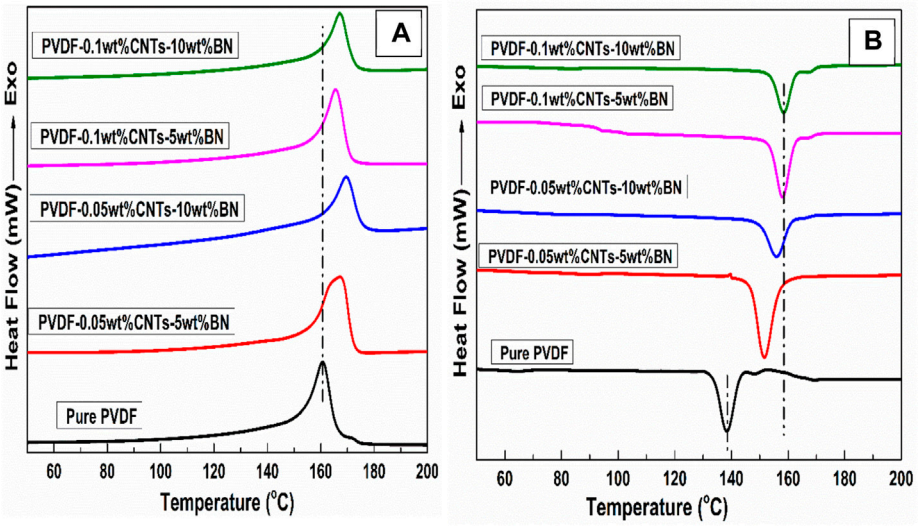

FIGURE 4
(A) Melting and **(B)** crystallization temperature of the nanocomposites.

as displayed in Figure 4A, which is about 8.87°C increase. Since there was no decrease in the T_m of the nanocomposites relative to the pure PVDF, the nanocomposites have no significant formation of small bundles or aggregate by the nanoparticles in the PVDF matrix which could have results to decrease in the T_m (Li et al., 2017). Also, all the nanocomposites had higher T_c compared to the pure PVDF. The T_c increased from 138.34°C for the pure PVDF to the range of 151.59°C–158.49°C depending on the nanocomposites as presented Figure 4B. This shows that crystallization of the nanocomposites started at higher temperature when compared with the pure PVDF due to the presence of the CNTs-BN which promoted heterogeneous nucleation. Although the introduction of CNTs-BN nanoparticles into the PVDF matrix increased its T_m more than its T_c, this indicates the effect of undercooling for crystallization to take place.

The degree of the undercooling ($\triangle T$) and percentage crystallinity (X_c) of the nanocomposites are presented in Table 2. Due to the heterogenous nucleation of the nanocomposites and increase in T_c, the $\triangle T$ is lower for all the nanocomposites compared to the pure PVDF. According to Li et al. (2017), the reduction in the $\triangle T$ is an indication of narrow distribution of crystallite size in the nanocomposites, while the pure polymer could have wide distribution of the crystallite size. This often results to lower driving energy for crystallization of the polymer matrix with addition of nanoparticles (Thomas and Zaikov, 2008; Jun et al., 2018), which is the major reason for the start of

TABLE 2 DSC properties of the nanocomposites.

Samples	Melting temperature T_m (°C)	Crystallization temperature T_c (°C)	Undercooling △T (T_m-T_c)	Percentage crystallinity X_c (%)
Pure PVDF	160.73	138.34	22.39	35.00
PVDF-0.05wt%CNTs-5wt%BN	167.19	151.59	15.60	36.77
PVDF-0.05wt%CNTs-10wt%BN	169.60	155.95	13.65	37.05
PVDF-0.1wt%CNTs-5wt%BN	165.55	158.03	7.52	36.86
PVDF-0.1wt%CNTs-10wt%BN	167.24	158.49	8.75	39.24

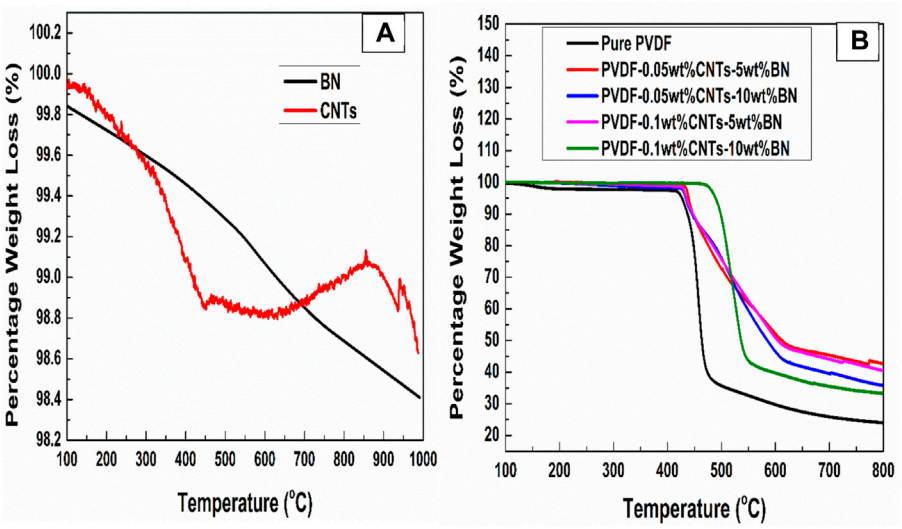

FIGURE 5
TGA curves of the **(A)** nanoparticles and **(B)** nanocomposites.

crystallization at higher temperature compared to the pure PVDF. This study recorded decreased in the △T from 22.39°C for the pure PVDF to the range of 15.60°C–7.52°C for various nanocomposites as depicted in Table 2. Although, the addition of CNTs and BN in the PVDF matrix could impede the regional growth of polymer chains (Mertens and Senthilvelan, 2018), the formation of many nucleation sites in the liquid matrix results to enhance crystalline phase and increase in X_c. Therefore, in this study, X_c increased from 35% for the pure PVDF to optimal of 39.24% for PVDF-0.05wt%CNTs-10wt%BN. Similar observation of the increment of X_c relative to that of pure polymer have been previously reported (Miltner et al., 2008; Kazemi et al., 2017).

The TGA curves of the BN and CNTs nanoparticles is presented in Figure 5A. The BN exhibits excellent thermal stability with only about 1.3 wt% loss up to 900°C. Other studies have also shown that up to that temperature range, BN has relatively little weight loss (Sudeep et al., 2015; Wu et al., 2019). On the other hand, CNTs typically have great thermal stability (Trakakis et al., 2013). In this study, CNTs also demonstrated its high thermal stability and good thermal resistance to disintegration. The thermal decomposition of the CNTs began around 88.3°C, which is attributed to the material's loss of water. The CNTs having oxygen functional groups demonstrated pyrolytic breakdown at 450°C with a weight loss of roughly 1.2 wt%. It only lost about 1 wt% of its weight at 900°C, which shows very excellent thermal stability. The thermal stability of the nanocomposites is represented in Figure 5B, which shows that all the nanocomposites moved to the high temperature compared to the pure PVDF. This was because of the larger amount of energy needed to break the interfacial bonds between the matrix and nanoparticles and cause the PVDF chains degrade (He et al., 2014).

The pure PVDF showed first thermal decomposition around 150°C and second major decomposition around 420°C. The nanocomposites showed major thermal decomposition above 440°C with optimal of about 475°C for PVDF-0.1wt%CNTs-10wt%BN nanocomposite, which is about 55°C increase in thermal stability. This implies that the degradation of the PVDF molecular chains at lower applied thermal energy was prevented by the CNTs and BN in the matrix. Hence, more thermal energy was absorbed by the nanocomposites before degradation. The pure PVDF also showed sharper slope of thermal decomposition

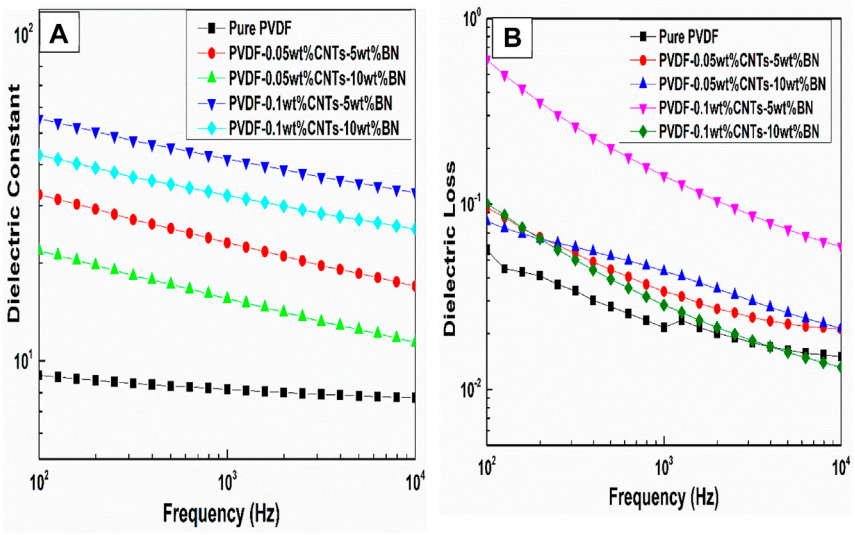

FIGURE 6
(A) Dielectric constant and **(B)** dielectric loss of the nanocomposites.

relative to the nanocomposites except the PVDF-0.1wt%CNTs-10wt%BN. Although this nanocomposite formulation shows higher starting of major thermal decomposition, it also revealed fast decomposition slope. This can be attributed to the higher content of the reinforcing phase compared to the other nanocomposites, which could have led to little formation of aggregates in the PVDF matrix. However, the general enhancement in thermal stability of the of nanocomposites can be credited to the good dispersion and interaction between the polymer matrix and the reinforcement phases as represented by the SEM micrograph in Figure 3 (Li et al., 2017). Since the BN and CNTs nanoparticles have good thermal stability as shown in Figure 5A, they offered thermal barriers in the matrix of the polymer, which slowed down the degradation of the nanocomposites (Nurul and Mariatti, 2013). In addition, the CNTs and BN have good capability of mechanically interlocking of the PVDF chains and restrict the flow of the chains on the application of heat, leading to improved thermal stability of the nanocomposites (Chu et al., 2012).

3.4 Dielectric constant and loss

The dielectric constant (ε^{I}) and dielectric loss (ε^{II}) of the nanocomposites are shown in Figure 6. A polymer matrix's characteristics such as dielectric properties are often modified by changing the microstructure of the matrix using reinforcement phase(s). The developed nanocomposites in this study showed significant rise in the ε^{I} due to the conductive nature of CNTs. As a result, when CNTs enter a polymer matrix, it significantly increases the ε^{I} of that polymer close to the percolative threshold (Ameli et al., 2013). On the other hand, various studies have also used BN to enhance the ε^{I} of polymeric materials (Wu et al., 2019; Zou et al., 2019). However, compared to CNTs, the ε^{I} enhancing potential of BN is often lesser due to its lower aspect ratio and insulative nature. To considerably improve the ε^{I} of the polymer in which such ceramic particles are incorporated, they need a high proportion (over 40 vol%) (Yoon et al., 2009), which has negative effect on mechanical properties of such polymer composites such as poor strength and flexibility. Hence, addition of small amount of conductive CNTs into the PVDF-BN system significantly improved the ε^{I} of the nanocomposites at a low fraction of BN.

For instance, ε^{I} at 100 Hz increased from about 9.1 for the pure PVDF to the range of 21.8 for PVDF-0.05wt%CNTs-10wt%BN and optimal of 55.4 for PVDF-0.1wt%CNTs-5wt%BN as shown in Figure 6A. This is a large range of improvement with the optimal of about 508.8% increase compared to the pure PVDF. There have been several theories linking the development of micro-capacitors in the polymer matrix to such increase in ε^{I} of the nanocomposites (Fan et al., 2012; Chu et al., 2013). This type of micro-capacitor is created in the polymer matrix by separating adjacent fillers with thin polymer layers to create sandwich structures that consist of conductor - insulator - conductor. Therefore, in the polymer matrix, several of these micro-capacitors can be created when the CNTs content increases with a larger increase in ε^{I}. This is most likely the cause of the high ε^{I} of the PVDF-0.1wt%CNTs-5wt%BN nanocomposite compared to others as the content of CNTs increase from 0.05wt% to 0.1wt% and BN decreased from 10wt% to 5wt%. At all the tested frequency range, the developed nanocomposites revealed higher ε^{I} than the pure PVDF. However, all the nanocomposites exhibited greater frequency dependence than the pure PVDF. This is because of the PVDF matrix and the nanoparticles having different polarization effects and dipole relaxation while achieving equilibrium at high frequency (Alhusaiki-Alghamdi, 2017).

The ε^{II} of the nanocomposites is shown Figure 6B, which reveals that the addition of the CNTs and BN to the polymer matrix caused an increase in the ε^{II}. However, the ε^{II} of the nanocomposites is relatively low (less than 1 for all the developed nanocomposites). For instance, the ε^{II} of about 0.06 was recorded for the pure PVDF, while 0.09, 0.08 and 0.1 at 100 Hz were measured for PVDF-0.05wt%CNTs-5wt%

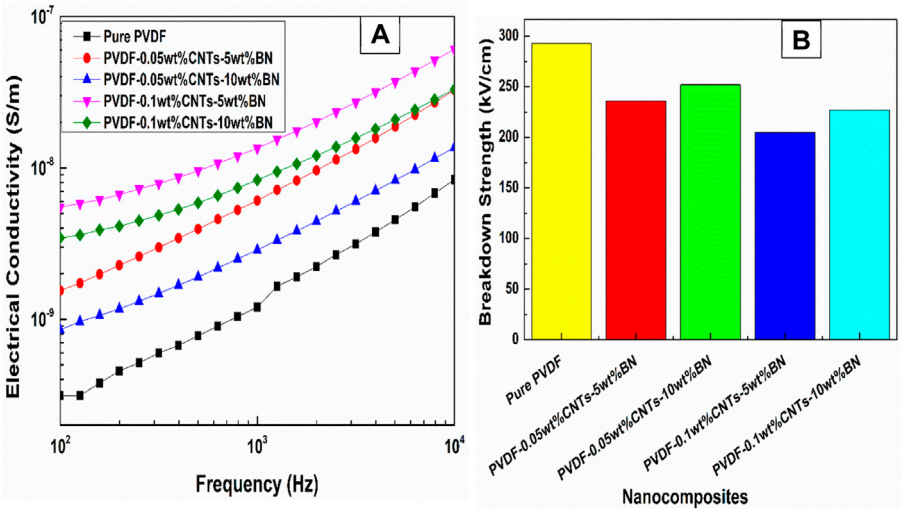

FIGURE 7
(A) Electrical conductivity and **(B)** breakdown strength of the nanocomposites.

BN, PVDF-0.05wt%CNTs-10wt%BN and PVDF-0.1wt%CNTs-10wt %BN respectively. The low ε^{II} of the nanocomposites can be credited to the incorporation of the insulation BN nanoparticles in the polymer matrix. This reduced the current leakage, fast mobility of charge carriers, trapping of charges at the interface of CNTs-BN, minimizing the migration of charge carriers from one CNTs to another, reduction of direct contact of CNTs, low formation conductive networks and increase in insulative barrier by the presence of BN in the PVDF matrix (Wan et al., 2017; Lakshmi et al., 2018). Among all the nanocomposites developed in this study, the ε^{II} was more pronounced for the PVDF-0.1wt%CNTs-5wt%BN nanocomposite due the higher conductive CNTs and low insulative BN content. This indicates that there was more interconnection among CNTs and 5wt% BN could not provide optimal insulative barrier for the 0.1wt% CNTs content. However, the ε^{II} of the developed nanocomposites is still relatively low, which can also be attributed to the use of the conductive CNTs at low concentration and the presence of BN. Hence, the nanocomposites exhibit improved ε^{I} and low ε^{II}, which indicate their energy storage and loss capabilities respectively. In general, while CNTs enhanced the energy storage capacity of PVDF, the BN lowered the energy loss capacity of the nanocomposites.

3.5 Electrical conductivity and breakdown strength

The measured electrical conductivity σ) of the nanocomposites is presented in Figure 7A. The addition of CNTs into polymer matrix often formed conductive network structures *via* interconnection of the nanoparticles (Szentes et al., 2012). This facilitates the movement of free electrons from one nanoparticle to another with significant increase in the σ. Once percolative threshold of such nanocomposites is reached, they show significant increase in the σ (Panwar et al., 2007; Deepa et al., 2013). In this study, it was observed that CNTs and BN in the PVDF matrix slight increased the σ of the nanocomposites to approximately one-fold compared to the pure PVDF. This can be credited to the good insulative property of BN, which relatively maintained the low σ of the PVDF that is required for dielectric materials. As stated earlier the BN minimized direct contact of CNTs, reduced formation of conductive network configurations and provided insulative barriers on the surfaces of the CNTs in the PVDF matrix. Hence, it is believed that the main contribution to the little increase in the σ of the nanocomposites is non-ohmic conduction (where charge carriers migrate from one CNTs to another through bulk insulative barrier). Therefore, increase in the σ from about 3.13×10^{-10} S/m for the pure PVDF to the range of 8.5×10^{-10} S/m to 5.5×10^{-9} S/m at 100 Hz for the nanocomposites were measured as shown in Figure 7A. The σ increased with increasing frequency due to the development of conductive grain boundaries at high frequency (Elashmawi et al., 2017). The dielectric breakdown strength (E_b) of the nanocomposites, which slight decreased with addition of CNTs and BN compared to the pure PVDF is shown in Figure 7B. This was expected since the CNTs is a conductive nanoparticles capable of forming conductive network structures in the matrix with increase in the flow of charge carriers. Although the presence of BN could supressed this effect, foreign bodies in a polymer matrix often lead to electric field distortion and enhancement with reduction in the E_b (Xiao and Du, 2016). In addition, due to the difference in surface energy and ε^{I} between the PVDF matrix and the nanoparticles, there is large chances of localized electric field accumulation and reduction in the E_b on the application of electric field (Huang et al., 2011). However, the reduction in E_b of the nanocomposites relative to the pure PVDF is small, which indicates that the nanocomposites maintained appreciably the good E_b of the PVDF. For instance, the E_b only reduced from 293 kV/cm for the pure PVDF to the range of 252 kV/cm for PVDF-0.05wt%CNTs-10wt%BN. The nanocomposites containing 0.1wt% CNTs and 5wt% BN has the lowest E_b of about 205 kV/cm as shown in Figure 7B.

4 Conclusion

Polymer nanocomposites reinforced with CNTs and BN were developed and characterized in this study. SEM analysis of the nanocomposites showed that the nanoparticles were homogeneously dispersed in the polymer matrix, which contributed to the enhanced properties. It was noted that the addition of the CNTs and BN in the PVDF matrix improved its T_m and T_c, indicating enhancement in thermal properties. This was attributed to the high thermal energy required to decompose the bond between the polymer matrix and the nanoparticles. The calculated X_c of the nanocomposites showed that the CNTs and BN could improve the X_c of the PVDF matrix due to the increase in their T_c resulting from heterogeneous nucleation. The TGA analysis revealed that the decomposition temperature of the nanocomposites shifted to the higher temperature compared to the pure PVDF. About 55°C increase in the thermal stability was achieved. The residual materials at the elevated temperature were higher for the nanocomposites compared to the pure PVDF. The developed PVDF-CNTs-BN nanocomposites showed increased ε^{l} of about 508.8 when related to the pure PVDF. The nanocomposites showed low ε^{ll} and appreciable E_b, which were close to that of the pure PVDF. The developed polymer dielectric nanocomposites exhibit good potentials for energy-power application.

Data availability statement

The original contributions presented in the study are included in the article/supplementary material, further inquiries can be directed to the corresponding author.

Author contributions

UU: Conceptualization, Methodology, Investigation, Formal analysis and Writing Original Draft AP: Supervision, Funding Acquisition, Review, Editing and Validation and Methodology OP: Supervision, Funding Acquisition and Resources and Project Administration.

Acknowledgments

We appreciate the Faculty of Engineering and the Built Environment and the Centre for Energy and Electric Power, Tshwane University of Technology, South Africa for their supports.

Conflict of interest

The authors declare that the research was conducted in the absence of any commercial or financial relationships that could be construed as a potential conflict of interest.

Publisher's note

All claims expressed in this article are solely those of the authors and do not necessarily represent those of their affiliated organizations, or those of the publisher, the editors and the reviewers. Any product that may be evaluated in this article, or claim that may be made by its manufacturer, is not guaranteed or endorsed by the publisher.

References

Adaval, A., Chinya, I., Bhatt, B. B., Kumar, S., Gupta, D., Samajdar, I., et al. (2022). Poly (vinylidene fluoride)/graphene oxide nanocomposites for piezoelectric applications: Processing, structure, dielectric and ferroelectric properties. *Nano-Structures Nano-Objects* 31, 100899. doi:10.1016/j.nanoso.2022.100899

Adaval, A., Subash, C., Shafeeq, V., Aslam, M., Turney, T. W., Simon, G. P., et al. (2022). A comprehensive investigation on the influence of processing techniques on the morphology, structure, dielectric and piezoelectric properties of poly (vinylidene fluoride)/Graphene oxide nanocomposites. *Polymer* 256, 125239. doi:10.1016/j.polymer.2022.125239

Alhusaiki-Alghamdi, H. M. (2017). Thermal and electrical properties of graphene incorporated into polyvinylidene fluoride/polymethyl methacrylate nanocomposites. *Polym. Compos.* 38, E246–E253. doi:10.1002/pc.23997

Ameli, A., Jung, P., and Park, C. (2013). Electrical properties and electromagnetic interference shielding effectiveness of polypropylene/carbon fiber composite foams. *Carbon* 60, 379–391. doi:10.1016/j.carbon.2013.04.050

Ansaloni, L. M. S., and de Sousa, E. M. B. (2013). Boron nitride nanostructured: Synthesis, characterization and potential use in cosmetics. *Mater. Sci. Appl.* 4 (1), 22–28. doi:10.4236/msa.2013.41004

Chu, C-C., White, K. L., Liu, P., Zhang, X., and Sue, H-J. (2012). Electrical conductivity and thermal stability of polypropylene containing well-dispersed multi-walled carbon nanotubes disentangled with exfoliated nanoplatelets. *Carbon* 50 (12), 4711–4721. doi:10.1016/j.carbon.2012.05.063

Chu, L., Xue, Q., Sun, J., Xia, F., Xing, W., Xia, D., et al. (2013). Porous graphene sandwich/poly(vinylidene fluoride) composites with high dielectric properties. *Compos. Sci. Technol.* 86, 70–75. doi:10.1016/j.compscitech.2013.07.001

Cortes, F. J. Q., and Phillips, J. (2015). Tube-super dielectric materials: Electrostatic capacitors with energy density greater than 200 J.cm(-3). *Mater. (Basel)* 8 (9), 6208–6227. doi:10.3390/ma8095301

Deepa, K. S., Gopika, M. S., and James, J. (2013). Influence of matrix conductivity and coulomb blockade effect on the percolation threshold of insulator–conductor composites. *Compos. Sci. Technol.* 78, 18–23. doi:10.1016/j.compscitech.2013.01.012

Du, M., Wang, W., Chen, L., Xu, Z., Fu, H., and Ma, M. (2016). Enhancing dielectric properties of poly(vinylidene fluoride)-based hybrid nanocomposites by synergic employment of hydroxylated BaTiO3and silanized graphene. *Polymer-Plastics Technol. Eng.* 55 (15), 1595–1603. doi:10.1080/03602559.2016.1163595

Elashmawi, I. S., Alatawi, N. S., and Elsayed, N. H. (2017). Preparation and characterization of polymer nanocomposites based on PVDF/PVC doped with graphene nanoparticles. *Results Phys.* 7, 636–640. doi:10.1016/j.rinp.2017.01.022

Fan, P., Wang, L., Yang, J., Chen, F., and Zhong, M. (2012). Graphene/poly(vinylidene fluoride) composites with high dielectric constant and low percolation threshold. *Nanotechnology* 23 (36), 365702–365708. doi:10.1088/0957-4484/23/36/365702

Han, K., Li, Q., Chen, Z., Gadinski, M. R., Dong, L., Xiong, C., et al. (2013). Suppression of energy dissipation and enhancement of breakdown strength in ferroelectric polymer–graphene percolative composites. *J. Mater. Chem. C* 1 (42), 7034–7042. doi:10.1039/c3tc31556h

He, Q., Yuan, T., Yan, X., Ding, D., Wang, Q., Luo, Z., et al. (2014). Flame-retardant polypropylene/multiwall carbon nanotube nanocomposites: Effects of surface functionalization and surfactant molecular weight. *Macromol. Chem. Phys.* 215 (4), 327–340. doi:10.1002/macp.201300608

Huang, C., Chen, C., Ye, X., Ye, W., Hu, J., Xu, C., et al. (2013). Stable colloidal boron nitride nanosheet dispersion and its potential application in catalysis. *J. Mater. Chem. A* 1 (39), 12192–12197. doi:10.1039/c3ta12231j

Huang, X., Jiang, P., and Tanaka, T. (2011). A review of dielectric polymer composites with high thermal conductivity. *IEEE Electr. Insul. Mag.* 27 (4), 8–16. doi:10.1109/mei.2011.5954064

Jang, J-U., Lee, S. H., Kim, J., Kim, S. Y., and Kim, S. H. (2021). Nano-bridge effect on thermal conductivity of hybrid polymer composites incorporating 1D and 2D nanocarbon fillers. *Compos. Part B Eng.* 222, 109072. doi:10.1016/j.compositesb.2021.109072

Jiang, Y., Shi, X., Feng, Y., Li, S., Zhou, X., and Xie, X. (2018). Enhanced thermal conductivity and ideal dielectric properties of epoxy composites containing polymer modified hexagonal boron nitride. *Compos. Part A Appl. Sci. Manuf.* 107, 657–664. doi:10.1016/j.compositesa.2018.02.016

Jin, X., Wang, J., Dai, L., Wang, W., and Wu, H. (2019). Largely enhanced thermal conductive, dielectric, mechanical and anti-dripping performance in polycarbonate/boron nitride composites with graphene nanoplatelet and carbon nanotube. *Compos. Sci. Technol.* 184, 107862. doi:10.1016/j.compscitech.2019.107862

Jun, Y-S., Um, J. G., Jiang, G., Lui, G., and Yu, A. (2018). Ultra-large sized graphene nano-platelets (GnPs) incorporated polypropylene (PP)/GnPs composites engineered by melt compounding and its thermal, mechanical, and electrical properties. *Compos. Part B Eng.* 133, 218–225. doi:10.1016/j.compositesb.2017.09.028

Karaphun, A., Tuichai, W., Chanlek, N., Sriwong, C., and Ruttanapun, C. (2021). Dielectric and electrochemical properties of hybrid Pt nanoparticles deposited on reduced graphene oxide nanoparticles/poly (vinylidene fluoride) nanocomposites. *Mater. Today Commun.* 27, 102232. doi:10.1016/j.mtcomm.2021.102232

Kazemi, Y., Kakroodi, A. R., Wang, S., Ameli, A., Filleter, T., Pötschke, P., et al. (2017). Conductive network formation and destruction in polypropylene/carbon nanotube composites via crystal control using supercritical carbon dioxide. *Polymer* 129, 179–188. doi:10.1016/j.polymer.2017.09.056

Lakshmi, N., Tambe, P., and Sahu, N. K. (2018). Giant permittivity of three phase polymer nanocomposites obtained by modifying hybrid nanofillers with polyvinylpyrrolidone. *Compos. Interfaces* 25 (1), 47–67. doi:10.1080/09276440.2017.1338876

Li, C-Q., Zha, J-W., Long, H-Q., Wang, S-J., Zhang, D-L., and Dang, Z-M. (2017). Mechanical and dielectric properties of graphene incorporated polypropylene nanocomposites using polypropylene-graft-maleic anhydride as a compatibilizer. *Compos. Sci. Technol.* 153, 111–118. doi:10.1016/j.compscitech.2017.10.015

Li, Y., Yang, W., Gao, X., Sun, R., and Wong, C-P. (2015). "Dielectric properties of CVD graphene/$BaTiO_3$/polyvinylidene fluoride nanocomposites fabricated through powder metallurgy," in *16th international conference on electronic packaging technology*. Paper presented at the 2015.

Maity, N., Mandal, A., and Nandi, A. K. (2016). Hierarchical nanostructured polyaniline functionalized graphene/poly(vinylidene fluoride) composites for improved dielectric performances. *Polymer* 103, 83–97. doi:10.1016/j.polymer.2016.09.048

Mertens, A. J., and Senthilvelan, S. (2018). Mechanical and tribological properties of carbon nanotube reinforced polypropylene composites. *J. Mater. Des. Appl.* 232 (8), 669–680. doi:10.1177/1464420716642620

Miltner, H. E., Grossiord, N., Lu, K., Loos, J., Koning, C. E., and Van Mele, B. (2008). Isotactic polypropylene/carbon nanotube composites prepared by latex technology. Thermal analysis of carbon nanotube-induced nucleation. *Macromolecules* 41 (15), 5753–5762. doi:10.1021/ma800643j

Min, C., Liu, D., Shen, C., Zhang, Q., Song, H., Li, S., et al. (2018). Unique synergistic effects of graphene oxide and carbon nanotube hybrids on the tribological properties of polyimide nanocomposites. *Tribol. Int.* 117, 217–224. doi:10.1016/j.triboint.2017.09.006

Nurul, M., and Mariatti, M. (2013). Effect of thermal conductive fillers on the properties of polypropylene composites. *J. Thermoplast. Compos. Mater.* 26 (5), 627–639. doi:10.1177/0892705711427345

Ouyang, W., Zeng, D., Yu, X., Xie, F., Zhang, W., Chen, J., et al. (2014). Exploring the active sites of nitrogen-doped graphene as catalysts for the oxygen reduction reaction. *Int. J. hydrogen energy* 39 (28), 15996–16005. doi:10.1016/j.ijhydene.2014.01.045

Panwar, V., Sachdev, V. K., and Mehra, R. M. (2007). Insulator conductor transition in low-density polyethylene–graphite composites. *Eur. Polym. J.* 43 (2), 573–585. doi:10.1016/j.eurpolymj.2006.11.017

Schmidt, D., Shah, D., and Giannelis, E. P. (2002). New advances in polymer/layered silicate nanocomposites. *Curr. Opin. Solid State Mater. Sci.* 6 (3), 205–212. doi:10.1016/s1359-0286(02)00049-9

Sudeep, P. M., Vinod, S., Ozden, S., Sruthi, R., Kukovecz, A., Konya, Z., et al. (2015). Functionalized boron nitride porous solids. *RSC Adv.* 5 (114), 93964–93968. doi:10.1039/c5ra19091f

Szentes, A., Varga, C., Horvath, G., Bartha, L., Kónya, Z., Haspel, H., et al. (2012). Electrical resistivity and thermal properties of compatibilized multi-walled carbon nanotube/polypropylene composites. *Express Polym. Lett.* 6 (6), 494–502. doi:10.3144/expresspolymlett.2012.52

Thomas, S., and Zaikov, G. E. (2008). *Polymer nanocomposite research advances*. New York, USA: Nova Science Publishers.

Trakakis, G., Tasis, D., Parthenios, J., Galiotis, C., and Papagelis, K. (2013). Structural properties of chemically functionalized carbon nanotube thin films. *Materials* 6 (6), 2360–2371. doi:10.3390/ma6062360

Uyor, U., Popoola, A., Popoola, O., and Aigbodion, V. (2019). Advancement on suppression of energy dissipation of percolative polymer nanocomposites: A review on graphene based. *J. Mater. Sci. Mater. Electron.* 30, 16966–16982. doi:10.1007/s10854-019-02079-1

Uyor, U. O., Popoola, A. P. I., Popoola, O. M., and Aigbodion, V. S. (2019). Enhanced thermal and mechanical properties of polymer reinforced with slightly functionalized graphene nanoplatelets. *J. Test. Eval.* 47 (4), 0336–2692. doi:10.1520/JTE20180336

Wan, Y-J., Zhu, P-L., Yu, S-H., Yang, W-H., Sun, R., Wong, C-P., et al. (2017). Barium titanate coated and thermally reduced graphene oxide towards high dielectric constant and low loss of polymeric composites. *Compos. Sci. Technol.* 141, 48–55. doi:10.1016/j.compscitech.2017.01.010

Wang, D., Bao, Y., Zha, J-W., Zhao, J., Dang, Z-M., and Hu, G-H. (2012). Improved dielectric properties of nanocomposites based on poly (vinylidene fluoride) and poly (vinyl alcohol)-functionalized graphene. *ACS Appl. Mater. interfaces* 4 (11), 6273–6279. doi:10.1021/am3018652

Wang, J., Shi, Z., Wang, X., Mai, X., Fan, R., Liu, H., et al. (2018). Enhancing dielectric performance of poly (vinylidene fluoride) nanocomposites via controlled distribution of carbon nanotubes and barium titanate nanoparticle. *Eng. Sci.* 4 (24), 79–86.

Wang, M., Jiao, Z., Chen, Y., Hou, X., Fu, L., Wu, Y., et al. (2018). Enhanced thermal conductivity of poly (vinylidene fluoride)/boron nitride nanosheet composites at low filler content. *Compos. Part A Appl. Sci. Manuf.* 109, 321–329. doi:10.1016/j.compositesa.2018.03.023

Weng, L., Wang, T., and Liu, L. (2017). A study on the structure and properties of poly(vinylidene fluoride)/graphite micro-sheet composite films. *J. Compos. Mater.* 51 (27), 3769–3778. doi:10.1177/0021998317693675

Wu, L., Wu, K., Lei, C., Liu, D., Du, R., Chen, F., et al. (2019). Surface modifications of boron nitride nanosheets for poly (vinylidene fluoride) based film capacitors: Advantages of edge-hydroxylation. *J. Mater. Chem. A* 7 (13), 7664–7674. doi:10.1039/c9ta00616h

Xiao, M., and Du, B. X. (2016). Review of high thermal conductivity polymer dielectrics for electrical insulation. *High. Volt.* 1 (1), 34–42. doi:10.1049/hve.2016.0008

Xihong, H. (2013). A review on the dielectric materials for high energy-storage application. *J. Adv. Dielectr.* 3 (1), 1330001–1330014. doi:10.1142/S2010135X13300016

Ye, H., Meng, N., Xu, C., Meng, Z., and Xu, L. (2018). High dielectric constant and low loss in poly (fluorovinylidene-co-hexafluoropropylene) nanocomposite incorporated with liquid-exfoliated oriented graphene with assistance of hyperbranched polyethylene. *Polymer* 145, 391–401. doi:10.1016/j.polymer.2018.05.002

Ye, H., Zhang, X., Xu, C., and Xu, L. (2019). Few-layer boron nitride nanosheets exfoliated with assistance of fluoro hyperbranched copolymer for poly (vinylidene fluoride-trifluoroethylene) nanocomposite film capacitor. *Colloids Surfaces A Physicochem. Eng. Aspects* 580, 123735. doi:10.1016/j.colsurfa.2019.123735

Yoon, J-R., Han, J-W., and Lee, K-M. (2009). Dielectric properties of polymer-ceramic composites for embedded capacitors. *Trans. Electr. Electron. Mater.* 10 (4), 116–120. doi:10.4313/teem.2009.10.4.116

Yu, J., Choi, H. K., Kim, H. S., and Kim, S. Y. (2016). Synergistic effect of hybrid graphene nanoplatelet and multi-walled carbon nanotube fillers on the thermal conductivity of polymer composites and theoretical modeling of the synergistic effect. *Compos. Part A Appl. Sci. Manuf.* 88, 79–85. doi:10.1016/j.compositesa.2016.05.022

Zhang, W-B., Zhang, Z-X., Yang, J-H., Huang, T., Zhang, N., Zheng, X-T., et al. (2015). Largely enhanced thermal conductivity of poly(vinylidene fluoride)/carbon nanotube composites achieved by adding graphene oxide. *Carbon* 90, 242–254. doi:10.1016/j.carbon.2015.04.040

Zou, D., Huang, X., Zhu, Y., Chen, J., and Jiang, P. (2019). Boron nitride nanosheets endow the traditional dielectric polymer composites with advanced thermal management capability. *Compos. Sci. Technol.* 177, 88–95. doi:10.1016/j.compscitech.2019.04.027